Micro-Continuum Modeling of Nuclear Waste Glass Corrosion

Fuel Cycle Research & Development

Prepared for
U.S. Department of Energy
Used Fuel Disposition Campaign
Carl I. Steefel
Lawrence Berkeley National Laboratory

August, 2014

FCRD-UFD-2014-000479

DISCLAIMER

This information was prepared as an account of work sponsored by an agency of the U.S. Government. While this document is believed to contain correct information, Neither the U.S. Government nor any agency thereof, nor the Regents of the University of California, nor any of their employees, makes any warranty, expressed or implied, or assumes any legal liability or responsibility for the accuracy, completeness, or usefulness, of any information, apparatus, product, or process disclosed, or represents that its use would not infringe privately owned rights. References herein to any specific commercial product, process, or service by trade name, trade mark, manufacturer, or otherwise, does not necessarily constitute or imply its endorsement, recommendation, or favoring by the U.S. Government or any agency thereof, or the Regents of the University of California. The views and opinions of authors expressed herein do not necessarily state or reflect those of the U.S. Government or any agency thereof or the Regents of the University of California

Revision 2
12/20/2012

APPENDIX E

FCT DOCUMENT COVER SHEET [1]

Name/Title of Deliverable/Milestone/Revision No.	Micro-Continuum Modeling of Nuclear Waste Glass Corrosion
Work Package Title and Number	Waste Form Degradation Modeling – LBNL FT-14LB080403
Work Package WBS Number	1.02.08.04
Responsible Work Package Manager	Carl I. Steefel (signature on file)
	(Name/Signature)

Date Submitted 08/12/2014

Quality Rigor Level for Deliverable/Milestone[2]	☐ QRL-3	☐ QRL-2	☐ QRL-1 ☐ Nuclear Data	☒ Lab/Participant QA Program (no additional FCT QA requirements)

This deliverable was prepared in accordance with Lawrence Berkeley National Laboratory
(Participant/National Laboratory Name)

QA program which meets the requirements of
☒ DOE Order 414.1 ☐ NQA-1-2000 ☐ Other

This Deliverable was subjected to:

☐ Technical Review ☐ Peer Review

Technical Review (TR)

Review Documentation Provided

☐ Signed TR Report or,
☐ Signed TR Concurrence Sheet or,
☐ Signature of TR Reviewer(s) below

Peer Review (PR)

Review Documentation Provided

☐ Signed PR Report or,
☐ Signed PR Concurrence Sheet or,
☐ Signature of PR Reviewer(s) below

Name and Signature of Reviewers

NOTE 1: *Appendix E should be filled out and submitted with the deliverable. Or, if the PICS:NE system permits, completely enter all applicable information in the PICS:NE Deliverable Form. The requirement is to ensure that all applicable information is entered either in the PICS:NE system or by using the FCT Document Cover Sheet.*

NOTE 2: *In some cases there may be a milestone where an item is being fabricated, maintenance is being performed on a facility, or a document is being issued through a formal document control process where it specifically calls out a formal review of the document. In these cases, documentation (e.g., inspection report, maintenance request, work planning package documentation or the documented review of the issued document through the document control process) of the completion of the activity along with the Document Cover Sheet is sufficient to demonstrate achieving the milestone. If QRL 1, 2, or 3 is not assigned, then the Lab/Participant QA Program (no additional FCT QA requirements box must be checked, and the work is understood to be performed, and any deliverable developed, in conformance with the respective National Laboratory/Participant, DOE- or NNSA-approved QA Program.*

This page is intentionally blank.

CONTENTS

FIGURES vi

ACRONYMS vi

1. INTRODUCTION 1

2. SUMMARY OF 25 YEAR FRENCH GLASS SON68 LEACHING EXPERIMENT 1

3. KINETIC-MICROSCOPIC-CONTINUUM MODEL (KμC) 3

4. MODEL SETUP FOR 25 YEAR FRENCH GLASS EXPERIMENT 4

5. SIMULATION RESULTS 5

6. DISCUSSION 7

7. ACKNOWLEDGEMENTS 10

8. REFERENCES CITED 11

FIGURES

Figure 1: Experimental setup for the 25 year SON68 glass leaching experiment (Guittonneau et al., 2011) 2

Figure 2: Schematic of modeling setup showing nanometer-scale reaction and diffusion zones. 5

Figure 3: Schematic of the disposition of elemental leaching zones based on atom probe tomography (from Gin et al., 2013). 5

Figure 4: High resolution histogram of elemental abundance across the pristine glass-hydrated glass interface (from Gin et al., 2013). 6

Figure 5: Simulation results using the KμC model. Note the position of the B release front further from the pristine glass than the Li-H interdiffusion front, in qualitative agreement with the observations. 8

Figure 6: Simulated corrosion front position versus time. Note the linear (constant) rate of front propagation. 9

Figure 7: Simulated distribution of amorphous silica reaction product at 2 and 5 years. 9

Figure 8: Schematic of modeling setup showing nanometer-scale reaction and diffusion zones using in silica boundary condition comparison (Figure 9). 9

Figure 9: Effect of silica concentration in external fluid at 3 years. In this run, the glass coupon begins at 50 nm (Figure 8), which indicates that almost no glass corrosion is predicted when the external solution is at saturation with amorphous silica. 10

ACRONYMS

APT	Atom Probe Tomography
EFTEM	Energy-Filtered Transmission Electron Microscopy
PRI	Passive Reactive Interface
SEM	Scanning Electron Microscopy
TST	Transition State Theory

1. INTRODUCTION

The purpose of this contribution is to report on preliminary nano-continuum scale modeling of nuclear waste glass corrosion. The focus of the modeling is an experiment involving a French glass SON68 specimen leached for 25 years in a granitic environment (Guittonneau et al., 2011; Gin et al., 2011; Gin et al., 2013). The 25 year experiment carried out by French scientists offers a unique opportunity to examine the controls on the rate of nuclear glass corrosion under controlled experimental conditions using a borosilicate glass of the kind widely considered for nuclear waste storage. The long term experiment makes it possible to move beyond the initial rate stage, with direct measurements of the longer term, residual rates of corrosion. Important in this regard is whether the rate of corrosion shows a parabolic dependence on time, as would be expected from a conventional diffusion model in which the reaction products (amorphous silica-rich gel) create a diffusion barrier that grows in width over time, or whether the time dependence is linear (Guittonneau et al., 2011). A linear dependence on time would call into question the model of a Passive Reactive Interface (PRI) presented by Cailleteau et al. (2008), although it does not entirely preclude such a model if the interface maintains a constant width over time (forming at the leading edge next to the pristine glass and dissolving at the trailing edge). The leachate concentration measurements collected every 56 days over 25 years by Guittonneau et al. (2011) provide data to constrain the long term corrosion rate and its time dependence.

Equally important for understanding the actual mechanisms involved was the use of high spatial resolution chemical profiling of the nuclear glass leach layer. In this regard, the width of the reaction zone constrains to some extent the mechanisms involved, since a sharp boundary is not compatible with models presented earlier in which leaching occurs by inter-diffusion over a significant width of the gel corrosion layer. In addition, the spatial ordering of concentration profiles (coincident or non-coincident) may offer constraint on the mechanisms involved (Gin et al., 2013).

In this report, we focus on capturing the nano-scale concentration profiles reported in Gin et al. (2013). Carrying out the numerical analysis all the way to 25 years would require a larger grid, albeit in one dimension, so this will be reported on in subsequent reports. We use a high resolution continuum model with a constant grid spacing of 1 nanometer to investigate the glass corrosion mechanisms. While the continuum assumption is a severe approximation given the fact that the pores themselves are close to this size, this is currently the only way we have to consider the longer spatial and time scales for this problem. In addition, it allows us to include full multicomponent chemistry (including precipitation and dissolution), something which is not possible with molecular modeling approaches (Bourg and Steefel, 2012).

2. SUMMARY OF 25 YEAR FRENCH GLASS SON68 LEACHING EXPERIMENT

Guittonneau et al. (2011) report on a 25.75-year leaching experiment designed to improve our understanding of the mechanisms controlling glass dissolution in geological disposal conditions. A SON68 glass block was leached in slowly renewed synthetic groundwater (at 90ºC, 100 bars) in contact with sand, granite and Ni–Cr–Mo alloy specimens. One hundred and sixty-three samples were collected over the entire duration of the experiment and were used to calculate the mean thickness of the altered glass (28 ±9 μm) and the glass dissolution rate. After several months, the corrosion rate remained very constant at 6 $x10^{-3}$ g m^{-2} d^{-1} over the 25 years of the experiment, which is about 20 times higher than the residual rate measured in a batch reactor at the same temperature. The glass alteration layers investigated by Scanning Electron Microscopy (SEM) at the end of the experiment, however, showed neither a homogeneous thickness nor a homogeneous morphology.

The location of the sampling valve (at half the height of the glass block) seems to divide the glass block into two parts. In the upper half (above the sampling valve), the general morphology of the alteration layer consists of a relatively simple and uniform gel with some secondary phases that include rare earth phosphates. The mean measured thickness of this alteration layer is 6.7 ±0.3 μm. However, in the lower half of the glass block, the gel layer is thicker, with a mean measured thickness of 81.3 ±1.1 μm. These results indicate that the chemistry of the leachate solution was not homogeneous, presumably due to the effects of local transport within the experimental reactor. This led the authors to conclude that rate of glass corrosion is very sensitive to the composition of the leachate solution close to the glass surface, and thus to the rate of water renewal (flow). The study clearly shows that the overall rate of corrosion (aside from the variations in corrosion rate presumably due to local transport effects) was constant (linear) over nearly 25 years.

While the Guittonneau et al. (2011) study presented important information on the bulk leaching rate of the nuclear glass specimen over 25 years, the ground-breaking study by Gin et al. (2013) on the SON68 glass specimen presented extremely high spatial resolution post-mortem chemical profiles using atom probe tomography (APT) and Energy-Filtered Transmission Electron Microscopy (EFTEM). The APT technique allows the 3D reconstruction of the elemental distribution at the reactive interphase with sub-nanometer precision. The results show that (1) Li from the glass and hydrogen from the solution exhibit anti-correlated 15 nm wide gradients located between the pristine glass and the hydrated glass layer, and (2) boron exhibits an unexpectedly sharp profile (~3 nm width) located just outside (away from the pristine glass interface) of the Li/H interdiffusion layer. The authors interpreted the sharp profile as being consistent with a dissolution front rather than a diffusion-controlled release of boron. As a result, the accessibility of water to the pristine glass could be the rate-limiting step under these conditions. More generally, these findings strongly support the importance of inter-diffusion coupled with hydrolysis of the pristine glass silicate network as the primary controls on the long-term dissolution rate. The primary objective of the nano-continuum approach presented here is to determine whether this conceptual model proposed by Gin et al. (2013) is supported by quantitative numerical modeling.

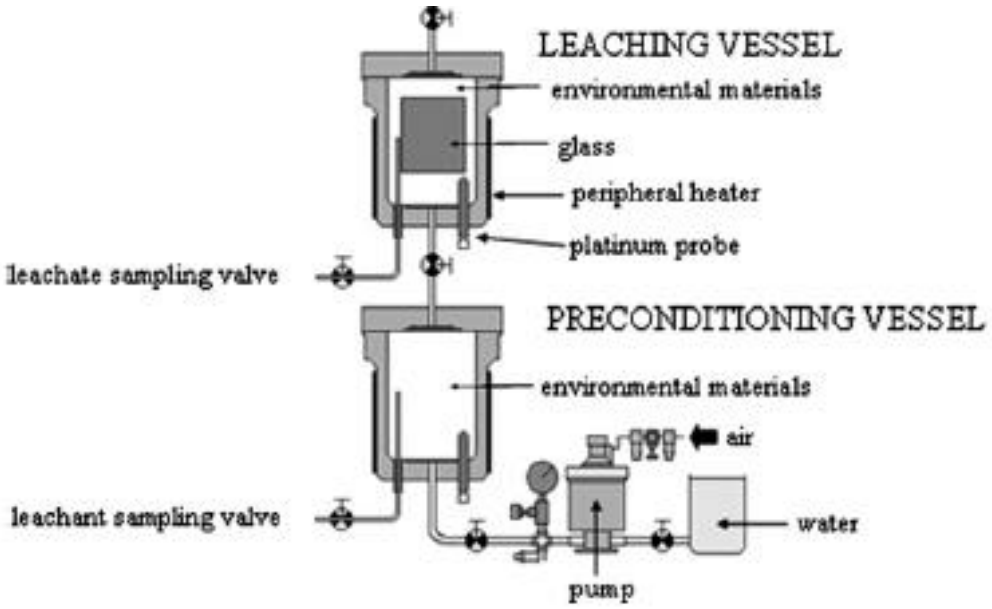

Figure 1: Experimental setup for the 25 year SON68 glass leaching experiment (Guittonneau et al., 2011)

3. KINETIC-MICROSCOPIC-CONTINUUM MODEL (KμC)

A new Kinetic Micro-Continuum (KμC) model for glass corrosion has been developed that avoids *a priori* assumptions about rate-limiting steps in the overall corrosion process. The KμC model provides a flexible approach in which individual parameters and processes are tunable, but in every case coupled within an overall dynamic framework. The KμC model may currently be run with either a single glass composition, which requires initially congruent dissolution, or it may be run with one or more glass end-member compositions that show differing thermodynamic and kinetic behavior. Since the single glass composition can be used to model overall incongruent reaction by incorporating rapid re-precipitation and/or ripening reactions, it is the preferred approach. The model currently includes the following processes

- Diffusion of water through the pristine glass and its alteration products;
- Ion exchange between water and the cations in the glass;
- Kinetically controlled hydrolysis reactions resulting in breaking of glass network bonds (Si, B, Al,…). The rate may be described by either a linear or a nonlinear TST law with an affinity control supplied by a specific phase (e.g., amorphous silica), or with an irreversible rate law with no affinity control. In either case, far from equilibrium dependencies of the rate on other dissolved (e.g., pH, Al, silica) or sorbed species can be included;
- Multicomponent diffusion of ions through the glass corrosion products;
- Precipitation reactions for amorphous and/or crystalline phases of variable composition that are kinetically and thermodynamically controlled;
- Kinetically controlled ripening and/or densification reactions that can reduce the porosity and/or pore connectivity (and thus the diffusivity) of the corrosion products;
- Kinetically and thermodynamically controlled formation of new crystalline phases (e.g., smectite, zeolite), with possible consequences for the transport properties of the corrosion layer;
- Flow and diffusion in the aqueous phase adjacent to the glass surface.

The KμC model incorporates the possibility of diffusion-limited glass corrosion by considering explicitly the kinetically-controlled densification of either (1) a residual silica-rich glass network in which other important components (e.g., the cations and network former boron) have been leached, or (2) of a newly precipitated silica-rich gel layer. However, in contrast to the GRAAL model (Frugier et al., 2008; Cailleteau et al., 2008), a diffusion-limited corrosion rate is not assumed *a priori* in the KμC model. Whether a passivating layer (i.e., defined as the *Passivating Reactive Interface* (PRI) by Frugier et al., 2008) forms in the KμC model depends on the relative rates of (1) silica recrystallization and densification, (2) leaching of the glass constituents, and (3) dissolution and/or recrystallization of the corrosion products.

The dissolution rate of the glass in the KμC model is not artificially limited by the approach to amorphous silica saturation (e.g., Grambow, 2006), although this formulation can be used if required. Thus, non-zero corrosion rates are allowed under conditions of silica saturation. Since the KμC model is formulated with an explicit treatment of multicomponent diffusion, kinetically-controlled mineral dissolution and precipitation, and glass corrosion, it can take into account the possibility that local chemical conditions within the nano- and micropores in the reaction products (i.e., the silica gel layer) may differ from conditions in the bulk solution adjacent to the corroding glass. In the absence of a reaction layer that limits diffusive transport to the pristine glass surface, silica saturation may not occur and the long-term rate of glass corrosion may remain high. In this case, the reduction in rate due to silica will be largely due to the ambient silica concentrations in the groundwater.

4. MODEL SETUP FOR 25 YEAR FRENCH GLASS EXPERIMENT

Ideally, the treatment of the corrosion of the SON68 glass over 25.75 years would involve a 3D analysis so as to capture the strong variations in the width of the corrosion zone on the glass surface within the experimental reactor. Clearly, there is some form of combined transport control at work here, potentially reflecting the role of both flow (the solution is renewed completely about once every five years, or at a rate of 22% of the total reactor porosity per year) and molecular diffusion. In addition to the 3D geometry, however, there is also the challenge of representing adequately the multiple scales involved here, with the experimental reactor involving scales of 10s of centimeters, while the corrosion layers on the glass require discretization on the order of nanometers. Since our preliminary focus is on capturing the width of the various reaction zones close to the pristine glass surface and their relative positions, we assume a pure diffusion-controlled regime and a constant grid spacing of 1 nanometer. The first 25 nanometers correspond to the granite and sand-filled zone upon which the SON68 rests. The assumption that a continuum model applies at this spatial scale is a severe approximation, given that pore sizes are close to this value, but the approach allows us to compare results with elemental profiles and avoids the additional requirement of a full computationally expensive and chemically simplified atomistic treatment.

As a boundary condition at one end of the reactor-glass specimen system, we consider a Dirichlet condition corresponding to the Volvic mineral water used to replenish periodically the experimental reactor (Guittonneau et al., 2011). The fixed concentration (Dirichlet) boundary condition is probably the best approximation to a flow-through system. At the other end of the 1D system, we assume a no-flux condition, which is reasonable as long as the corrosion front does not fully penetrate the glass specimen. Within the first 25 nanometers of the reaction, the system is characterized by a porosity of 0.41 (as in the experimental system reported by Guittonneau et al., 2011) and a mixture of quartz sand and granite. A diffusivity of 10^{-11} m^2/s for all ions was assumed for the sand-granite mixture. The alloy specimens included in the experiments were not considered in the modeling. From 25 nanometers out to 225 nanometers, the system was assumed to consist of a SON68 borosilicate glass with a porosity of 1%. The diffusivity of the borosilicate glass was assumed to follow a threshold type of model (Navarre-Sitchler et al., 2009), with a value of 10^{-23} m^2/s (in approximate agreement with the value proposed by Gin et al., 2013) for values of the porosity below 30% and a value of 10^{-11} m^2/s for porosity values above 30%. Modeling carried out earlier (Navarre-Sitchler et al., 2011) indicate that a simple porosity dependence, as in an unmodified Archie's Law formulation, cannot replicate the observed concentration profiles, since the reaction front continuously widens due to the simulated porosity and diffusivity enhancement. Some form of a threshold model, based on the idea that dissolution and porosity enhancement increase the rate of diffusivity by increasing connectivity (Navarre-Sitchler et al., 2009; 2011), appears to be required.

The dissolution of the glass is assumed to follow an affinity rate law (Grambow, 2006), but with a cubic dependence on the saturation state (departure from equilibrium) with respect to amorphous silica. A linear Transition State Theory (TST) dependence does not capture the sharp B front and places the B (and Na) dissolution front closer to the Li-H interdiffusion front. The rate of glass corrosion, in addition to following a cubic dependence on the departure from equilibrium, also depends on the hydration state of the glass. In other words, if the H_2O diffusion front has not yet penetrated the pristine glass, the rate is effectively zero. So the rate law used is given by

$$R_{corr} = k a_{H-hydrated}^{5} \left(1 - \frac{Q_{am-silica}}{K_{am-silica}} \right)^{3} \tag{1}$$

where k is the rate constant and $a_{H\text{-}hydrated}$ is the concentration of hydrated sites in the glass, and $Q_{am\text{-}silica}$ and $K_{am\text{-}silica}$ are the ion activity products and equilibrium constants with respect to amorphous silica. A higher-order dependence on the concentration of hydrated sites in the borosilicate glass is also required so as to locate the boron release front further from the Li-H interdiffusion front. This formulation could be

reconciled with a model in which the number of hydrated sites needs to reach some threshold value before the dissolution of the glass accelerates appreciably.

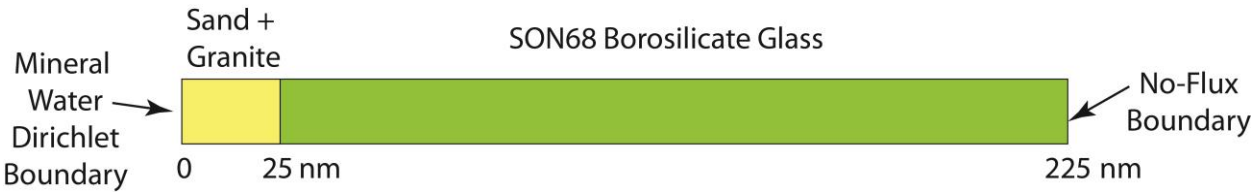

Figure 2: Schematic of modeling setup showing nanometer-scale reaction and diffusion zones.

5. SIMULATION RESULTS

In the simulations presented here, we present a semi-quantitative comparison of the modeling results and the data. In the modeling, concentration in the pore solution, rather than in the glass, is presented, so a quantitative comparison is not possible. The focus is on the relative position of the fronts, and in general, the width of the fronts as they evolve over time. Schematically, the geometry that we wish to capture in the modeling is given in Figure 3 taken from Gin et al. (2013). Most important is the relatively constant width of the reaction zones and the position of the sharp boron profile further from the pristine glass interface than is the Li-Water inter-diffusion zone. A more detailed Atom Probe Tomography (APT) profile from Gin et al. (2013) is given in Figure 4.

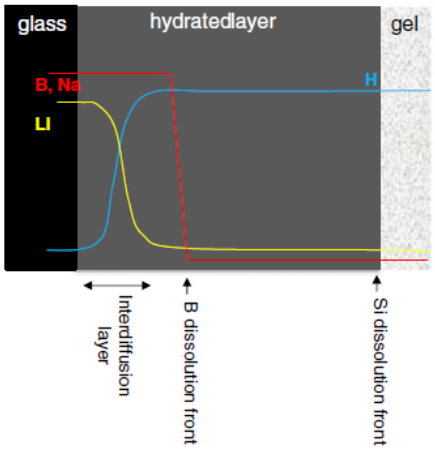

Figure 3: Schematic of the disposition of elemental leaching zones based on atom probe tomography (from Gin et al., 2013).

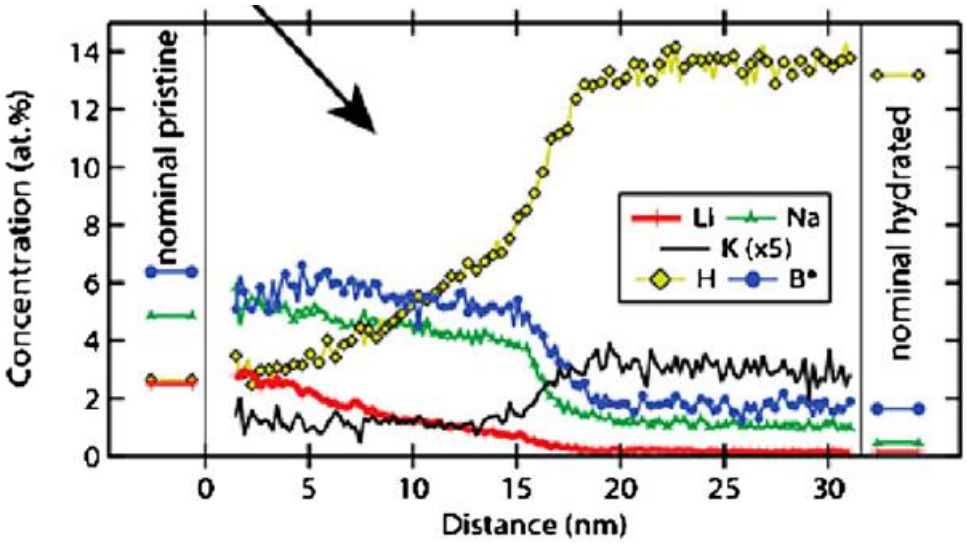

Figure 4: High resolution histogram of elemental abundance across the pristine glass-hydrated glass interface (from Gin et al., 2013).

The model results for the 1D run are shown in Figure 5 over a period of 4 years. Larger times than these require extending the grid (and the borosilicate glass) to larger distances, which will be presented in subsequent reports. The modeling results show that both the Li-H inter-diffusion front and the B release (dissolution) front are relatively sharp, and remain so over the course of the 4 year simulation. In addition, the B release front is located further from the pristine glass interface than is the Li-H inter-diffusion front, which makes sense insofar as the dissolution of the glass is promoted by its hydration.

In addition, the simulations predict a linear rate of front propagation over time once the initial period (less than 1 year) is passed (Figure 6). This can be explained by the maintenance of a constant-width zone over which diffusion is limiting (in agreement with the results of Navarre-Sitchler et al., 2011). Again, if the silica-rich gel layer were limiting, the dependence on time would be parabolic since this zone grows with time (Figure 7).

Another potential effect has to do with the concentration of the external pore fluid, which is particularly important since the glass coupon in the 26 year experiment shows very different corrosion rates depending on position within the reactor. In these simulations, the grid spacing has been changed so that the glass coupon begins at 50 nm (as in Figure 8, in contrast to the 25 nm shown in Figure 2). Since the external fluid in the reactor was not well-mixed, it appears that diffusion gradients developed within the reactor. If the concentration of silica in particular (the principal component known to inhibit glass corrosion) is lower close to the preconditioning vessel where the corrosion distances were greatest, then this suggests that slower corrosion rates at the top of the reactor may have been due to higher silica concentrations there. Using the KμC model, we compare in Figure 9 two different runs, one with 10 μM silica in the preconditioning vessel, one with the preconditioning vessel fixed at amorphous silica saturation for the run conditions (1936 μM). In this run, the glass coupon begins at 50 nm, so the amorphous silica boundary condition results in very little glass corrosion. In contrast, corrosion depths are greater in the case of the 10 μM silica boundary condition.

6. DISCUSSION

To the extent that the simulations agrees with the observations of the sharpness of the reaction fronts, the non-coincidence of the B and Li-H fronts, and the constant (linear) rate of corrosion, they support the conceptual model proposed by Gin et al. (2013). The rate-limiting step for corrosion appears to be the rate of diffusion of H (via water) into the pristine glass. The slow rate of diffusion, which is approximately 10^{-23} m^2/s, controls the overall rate of glass corrosion. An explicit Passive Reactive Interface (PRI) zone is not required. Moreover, the linear rate that is predicted by the simulations follows from the fact that the amorphous silica gel corrosion layer that forms on the glass is not itself a diffusion barrier. If it were, one would observe a parabolic dependence on time for the corrosion rate in the simulations and experiments, since the width of the diffusion barrier would grow with time in this case (Figure 7). A linear rate of advance is only possible when the width of the diffusion barrier remains approximately constant, in agreement with Navarre-Sitchler et al. (2011).

The conceptual model for glass corrosion based on modeling of these experiments needs to involve one in which H diffusion into the glass is coupled to glass dissolution. Once the glass is hydrated, the rate of dissolution is relatively fast, as indicated by the relatively large rate constants required, as well as by the sharpness of the dissolution front. Before hydration occurs, however, the borosilicate glass corrosion is effectively zero. So the proposed model is one in which diffusion into the pristine glass, which leads to hydration and ion exchange, is coupled to glass corrosion. The rate must depend on the extent of hydration (going from effectively zero at low hydration to very high rates when hydration is more nearly complete).

Another effect explored here has to do with the effect of the chemical composition of the external diffusion, effectively the boundary condition for the diffusion-reaction calculations. The major effect is likely to be from silica concentration based on previous studies documenting its inhibiting effect on corrosion. Since dramatically different corrosion rates were observed on the SON68 glass coupon as a function of position within the reactor, with the slowest rates observed at the top farthest from the connection to the preconditioning vessel (Figure 1), it appears that strong chemical gradients developed in the reactor (which was not mixed). The simulations presented here in Figure 9 support the idea that solution compositions closer to equilibrium with respect to amorphous silica will result in slower glass corrosion rates. This highlights the importance of coupling performance assessment models of glass corrosion with larger scale, even far-field calculations that are needed to provide the boundary conditions for the waste packages.

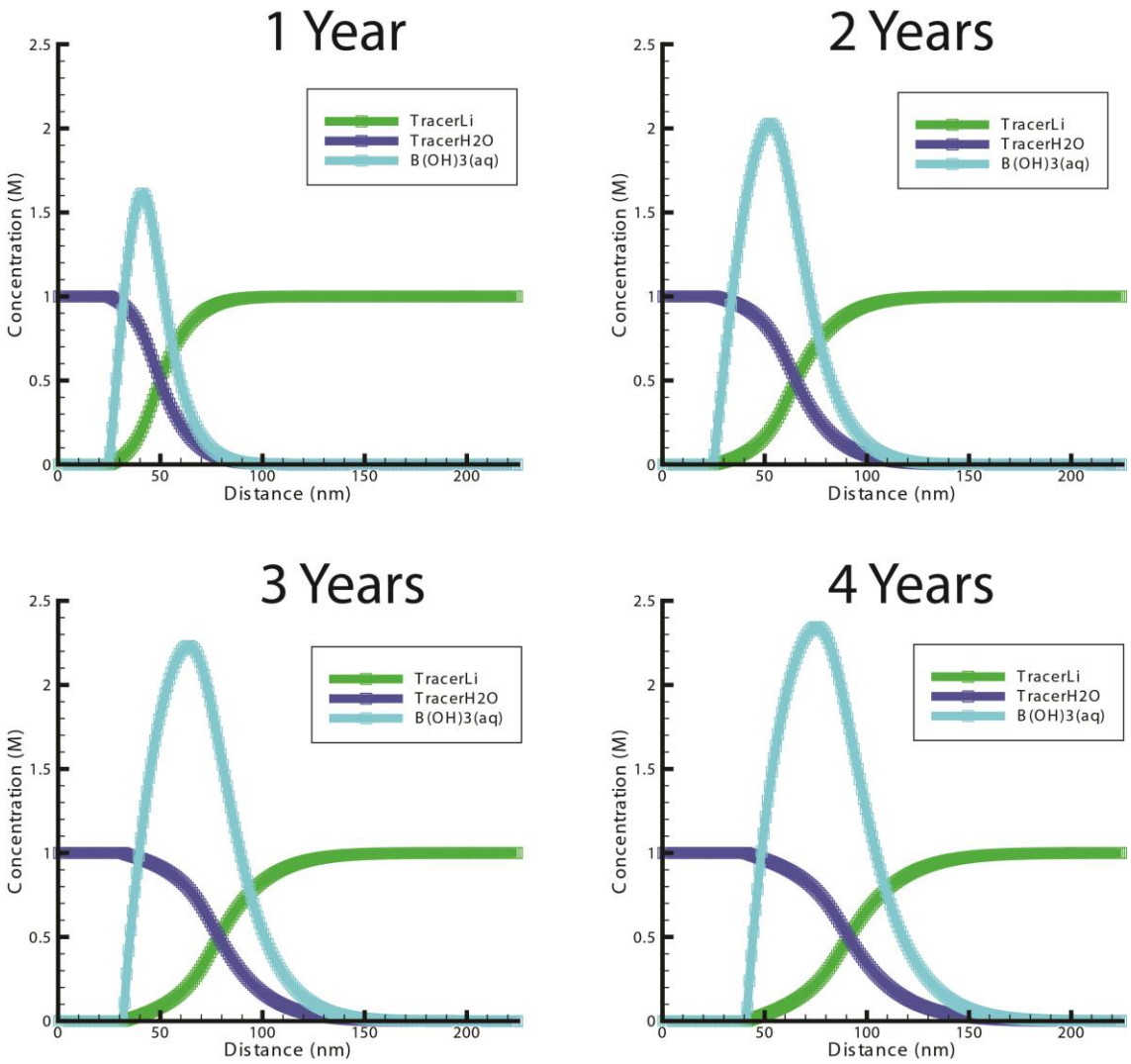

Figure 5: Simulation results using the KμC model. Note the position of the B release front further from the pristine glass than the Li-H interdiffusion front, in qualitative agreement with the observations.

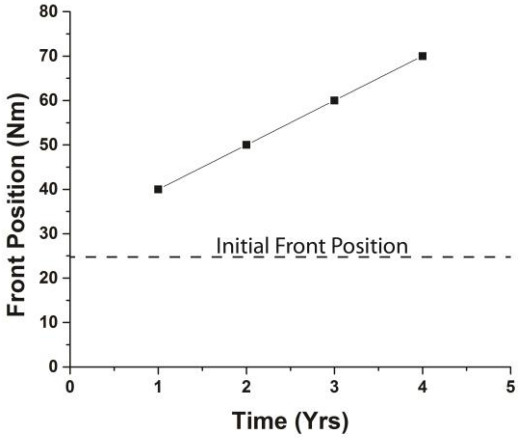

Figure 6: Simulated corrosion front position versus time. Note the linear (constant) rate of front propagation.

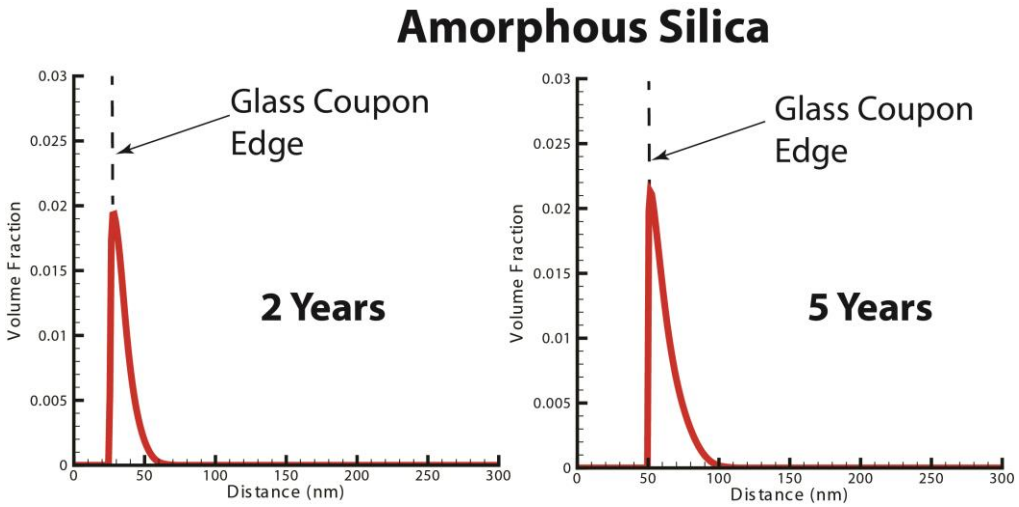

Figure 7: Simulated distribution of amorphous silica reaction product at 2 and 5 years.

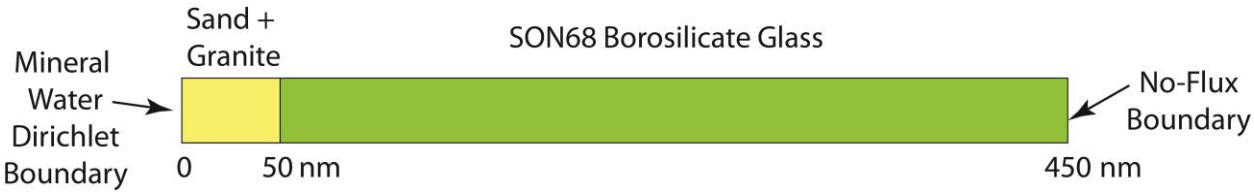

Figure 8: Schematic of modeling setup showing nanometer-scale reaction and diffusion zones using in silica boundary condition comparison (Figure 9).

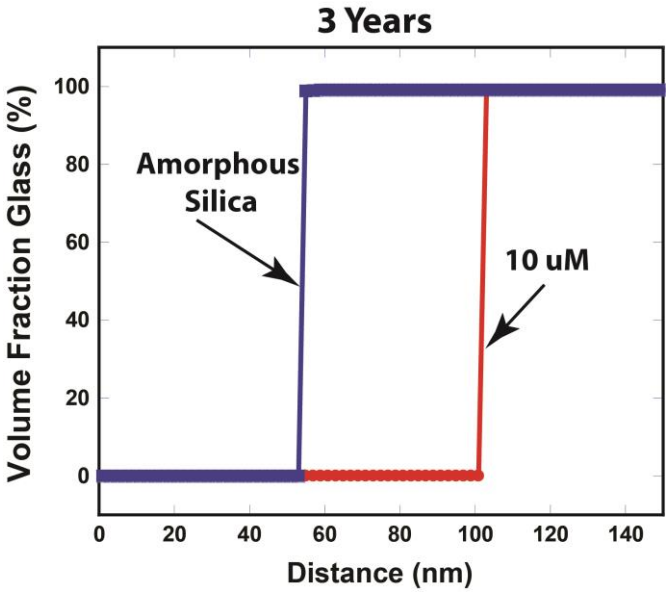

Figure 9: Effect of silica concentration in external fluid at 3 years. In this run, the glass coupon begins at 50 nm (Figure 8), which indicates that almost no glass corrosion is predicted when the external solution is at saturation with amorphous silica.

7. ACKNOWLEDGEMENTS

This work was supported by the U.S. Department of Energy Nuclear Energy Department, Separations and Waste Form Program. Subsequent funding has been provided by the Used Fuel Disposition Program within U.S. DOE Nuclear Energy. The work was carried out at Lawrence Berkeley National Laboratory under Contract No. DE-AC02-05CH11231.

8. REFERENCES CITED

Bourg, I.C., C.I. Steefel (2012). Molecular dynamics simulations of water structure and diffusion in silica nanopores. *J. Phys. Chem., **C*** **116**, 11556-11564.

Cailleteau C., F. Angeli, F. Devreux, S. Gin, J. Jestin, P. Jollivet, O. Spalla (2008). Insight into silicate-glass corrosion mechanisms. *Nature Materials,* **7**, 978-983.

Frugier P., S. Gin, Y. Minet, T. Chave, B. Bonin, N. Godon, J-E. Lartigue, P. Jollivet, A. Ayral, L. De Windt, G. Santarini (2008). SON68 nuclear glass dissolution kinetics: Current state of knowledge and basis of the new GRAAL model, *Journal of Nuclear Materials,* **380**, 8-21.

Grambow, B. (2006). Nuclear waste glasses – How durable? *Elements,* **2**, 357-364.

Gin S., J.Y. Ryan, D.K. Schreiber, J. Neeway, D. Cabie (2013). Contribution of atom-probe tomography to a better understanding of glass alteration mechanisms: Application to a nuclear glass specimen altered 25 years in a granitic environment. *Chemical Geology,* **349-350,** 99-109.

Gin S., C. Guittonneau, N. Godon, D. Neff, D. Rebiscoul, M. Cabie, S. Mostefaoui (2011). Nuclear glass durability: New insight in alteration layer properties. *Journal of Physical Chemistry, C **115***, 18696-19706.

Guittonneau, C., S. Gin, N. Godon, J.P. Mestre, O. Dugne, P. Allegri (2011). A 25-year laboratory experiment on French SON68 nuclear glass leached in a granitic environment—First investigations. *Journal of Nuclear Materials,* **408**, 73-89.

Navarre-Sitchler A., C.I. Steefel, L. Yang, L. Tomutsa, S.A. Brantley (2009). Evolution of porosity and diffusivity associated with chemical weathering of a basalt clast. *Journal of Geophysical Research,* **114**, DOI:10.1029/2008JF001060.

Navarre-Sitchler, A., C.I. Steefel, P.B. Sak, S.L. Brantley (2011). A reactive transport model for weathering rind formation on basalt. *Geochimica Cosmochimica Acta,* **75,** 7644-7667.